**Summary:** This investigation presents a simultaneous and convenient approach to produce a high-performance polyimide with a low dielectric constant by introducing the octa-acrylated polyhedral oligomeric silsesquioxane (methacrylated-POSS) into a polyimide matrix to form polyimide semi-interpenetrating polymer network (semi-IPN) nanocomposites. The differential scanning calorimetry (DSC) and Fourier-transform infrared (FT-IR) results indicate that the self-curing of methacrylated-POSS and the imidization of polyamic acid (PAA) occurs simultaneously. The morphology of a semi-IPN structure of polyimide/POSS-PI/POSS nanocomposites with POSS nanoparticles embedded inside the matrix is elucidated. The POSS particles are uniform and are aggregated to a size of approximately 50–60 nm inside the polyimide matrix. The interconnected POSS particles are observed at high POSS content. The structure is highly cross-linked, so the PI/POSS nanocomposites have an enhanced glass transition temperature. The high porosity of the PI/POSS nanocomposites markedly reduces the dielectric constant of PI because of the nanometer-scale porous structure of POSS.
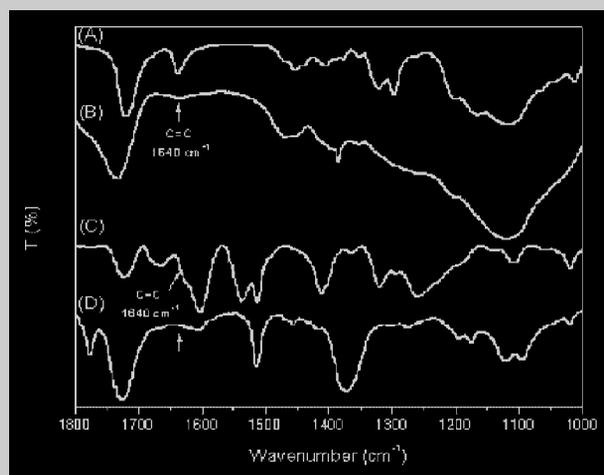
FT-IR spectra of the various compounds of A) methacrylate-POSS before curing, B) methacrylate-POSS after curing, C) PAA containing 15 wt.-% POSS, and D) PI/POSS containing 15 wt.-% POSS.

Simultaneous Preparation of PI/POSS Semi-IPN Nanocomposites

Wen-Yi Chen,[1] Ko Shan Ho,[2] Tar-Hwa Hsieh,[2] Feng-Chih Chang,[3] Yen-Zen Wang[1]*

[1] Department of Chemical Engineering, National Yun-Lin University of Science and Technology, 640, Yun-Lin, Taiwan ROC
Fax: 886-5-5312071; E-mail: wangzen@yuntech.edu.tw
[2] Department of Chemical and Material Engineering, National Kaohsiung University of Applied Sciences, 807, Kaohsiung, Taiwan ROC
[3] Institute of Applied Chemistry, National Chiao Tung University, 300, Hsinchu, Taiwan ROC

Introduction

Polyimides with a low dielectric constant (low k PIs) are polymers that are extensively used in microelectronics owing to their outstanding key properties such as thermoxidative stability, size stability, high thermal properties, high mechanical strength, and excellent electrical properties. Low k PIs are generally investigated by introducing fluorine atoms into the backbone of the polyimide or by introducing porosity into the polyimide matrix.[1−6] Both of these routes to reduce the dielectric constant of polyimide include several complicated steps to prepare precursors of the polyimide followed by a casting process to yield the low

k PIs. Semi-interpenetrating polymer networks (semi-IPNs) are known to be able to remarkably suppress the creep and flow of polymers.[7] The entanglement of different polymers considerably reduces the mobility of the individual polymer molecules in the semi-IPNs. Previous investigations[8−10] have shown that the sol−gel components or derivatives of poly(silsesquioxane) can be employed to prepare various polyimide matrices to form semi-IPN-like nanocomposites. However, some critical issues, including the dielectric constant of, the size stability of, and the problem of silica aggregation in the polyimide matrix are important challenges for material scientists. Polyhedral oligomeric silsesquioxane (POSS) derivatives are used in

the polyimide matrix to solve these problems. Many studies[11−13] have established that POSS derivatives efficiently enhance thermal, mechanical, and dielectric properties (low *k*) when they are introduced into the polymer backbone. Acrylate monomers have been applied to create a cross-linked structure in IPN or semi-IPN systems. The IPNs in the acrylate system can be formed by three routes: 1) thermal curing of various multiple acrylate monomers at high temperature (>100 °C), 2) the thermally initiated (by 2,2′-azoisobutyronitrile (AIBN), benzoyl peroxide (BPO)) polymerization of acrylate monomers to form networks,[14−17] and 3) the photoinitiated curing of acrylate monomers to yield networks through UV irradiation.[14]

This investigation reports that methacrylated-POSS can be easily introduced into the polyimide matrix to generate a PI/POSS semi-IPN-like nanocomposite. The methacrylated-POSS is the best candidate, because of the presence of multiple reactive groups (C=C), and the rigid, bulky, and porous structure. Therefore, the highly cross-linked structure derived from C=C self-curing and the porous structure of the methacrylated POSS can restrict the motion of polyimide molecules, which enhances the thermal, mechanical, and dielectric (low *k*) properties. In further work, the methacrylated-POSS will be extensively applied to yield IPN and semi-IPN nanocomposites with various other polymers by self-curing, thermal initiation, and photoinitiation.

Experimental Part

Materials

Methacrylated-POSS was purchased from Hybrid Plastics Company (Fountain Valley, CA). Pyromellitic dianhydride (PMDA) and 4,4′-methylenedianiline (MDA) were purchased from TCI in Tokyo, Japan.

Preparation of Polyamic Acid (PAA) Solution Containing Methacrylated POSS

A PAA solution that contained methacrylated-POSS (PMDA/MDA/methacrylated POSS) was prepared by the following steps: The desired amount of methacrylated-POSS and 10.00 mmol of MDA were fed into a three-necked flask that contained 22.92 g of dimethylacetamide (DMAc) under nitrogen purging at 25 °C. After the MDA was dissolved, 10.20 mmol of PMDA was divided into three batches, and added to the flask batch-by-batch at intervals of 0.5 h. When the PMDA was completely dissolved, the solution was stirred continuously for 1 h, a viscous PAA solution was obtained. The mixture was further agitated for an additional 12 h using a mechanical stirrer. The final content of PAA in DMAc was 11 wt.-%.

Preparation of PI/POSS Semi-IPN Nanocomposites

A PAA solution that contained methacrylated-POSS was cast on a glass slide, using a doctor blade. It was then placed in a vacuum oven at 40 °C for 48 h before imidization. The PMDA/MDA/methacrylated-POSS mixture was completely imidized by storing the sample in an oven in which air was circulated at 100, 150, 200, and 250 °C for 1 h, and then at 300 °C for 0.5 h, to ensure complete imidization.

Characterization

The self-curing of methacrylated-POSS was examined using a DuPont differential scanning calorimeter (DSC Q100) in an atmosphere of nitrogen. The sample was placed on a KBr pellet and the FT-IR spectrum was obtained using a Nicolet AVATAR 320 FT-IR spectrometer. The glass transition temperature was obtained using a DuPont dynamic mechanical analyzer (DMA Q800) and the thermal stabilities were studied using a DuPont thermogravimetric analyzer (TGA Q500) under flowing nitrogen. The dielectric constant was measured using a DuPont dielectric analyzer (DEA 2970). The coefficients of thermal expansion (CTE) of the films were determined using a DuPont thermomechanical analyzer (TMA 2940) film probe. An X-ray diffraction (XRD) study of the sample was performed using a MAC Science MXP18 X-ray diffractometer (40 kV, 200 mA) with a copper target at a scanning rate of 4 deg · min^{-1}. Field-emission scanning electron microscopy (FE-SEM) observations were made using a JEOL 5300 microscope.

Results and Discussion

Characterization of Self-Curing of Methacrylated-POSS and Chemical Structure of PI/POSS Nanocomposites

The C=C self-curing of methacrylated-POSS and imidization of PAA can be characterized by DSC and FT-IR spectroscopy. Figure 1 displays DSC thermograms of neat methacrylated-POSS, neat PAA, and PAA that contains 15 wt.-% POSS. The initial curing temperature of methacrylated-POSS is 160 °C and the heat flow peak is 318 °C. The DSC profile of PAA exhibits an endothermic peak at 155 °C (DMAc evaporation) and the initial imidization temperature of PAA is 159 °C. The DSC thermogram of PAA that contains 15 wt.-% POSS closely matches that of pure PAA. Figure 2(A) and (B) show the FT-IR spectra of methacrylated-POSS before and after curing, respectively. The main peaks of C=C at 1 640 cm^{-1} and Si–O–Si at 1 100 cm^{-1} are assigned to methacrylated-POSS. Curing significantly reduces the main peak (1 640 cm^{-1}) of the C=C group of methacrylated-POSS, which verifies the self-curing of methacrylated-POSS. Figure 2(C) and (D) show the FT-IR spectra of the PAA that contains 15 wt.-% POSS and a nanocomposite of PI/POSS-15 wt.-%, respectively. A PAA that contains the methacrylated-POSS structure is characterized by absorption bands at 1 640 (C=C, in methacrylated-POSS), 1 667 (C=O, in the amide group), 1 538 (C–N, in the amide group), and 1 100 cm^{-1} (Si–O–Si, in the POSS cage).[18] Following the reaction, complete imidization is verified by the absorption bands at 1 777 (asymmetric
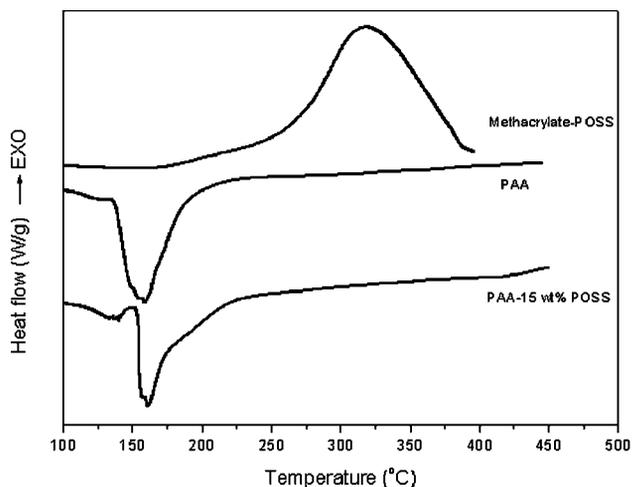
Figure 1. DSC thermograms of methacrylate-POSS, PAA, and PAA containing 15 wt.-% POSS under nitrogen atmosphere.

C=O in the imide group) and $1\,725\ cm^{-1}$ (symmetric C=O in the imide group),[18] and by the absence of the bands at $1\,640$, $1\,667$, and $1\,538\ cm^{-1}$. Therefore, a highly cross-linked PI/POSS semi-IPN nanocomposite had already been obtained. The DSC and FT-IR results demonstrate that the process conveniently yields a high-performance nanocomposite based on PI/POSS semi-IPN nanocomposites.

Morphology

Several studies have reported the morphologies of polymers that contain various functional POSSs.[19−23] This investigation develops a POSS dispersed in a semi-IPN system. XRD and FE-SEM are employed to elucidate the dispersion of methacrylated-POSS in PI/POSS nanocomposites. Figure 3 presents the XRD profiles of PI/POSS semi-IPN nanocomposites. The polyacrylated-POSS monomer is liquid-like and corresponding networks that contain POSS
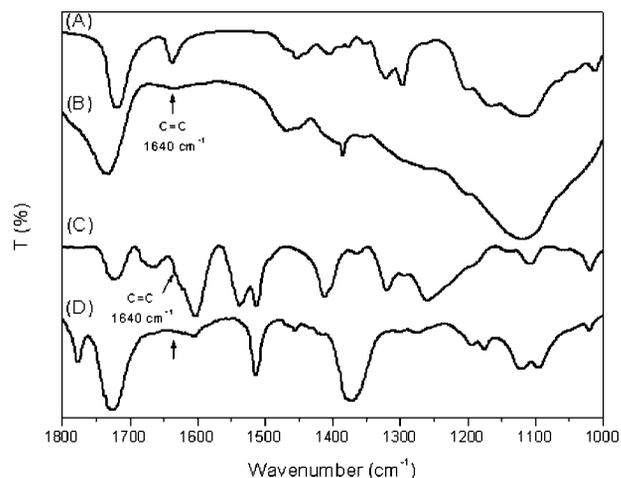

Figure 2. FT-IR spectra of: A) methacrylate-POSS before curing, B) methacrylate-POSS after curing, C) PAA containing 15 wt.-% POSS, and D) PI/POSS containing 15 wt.-% POSS.
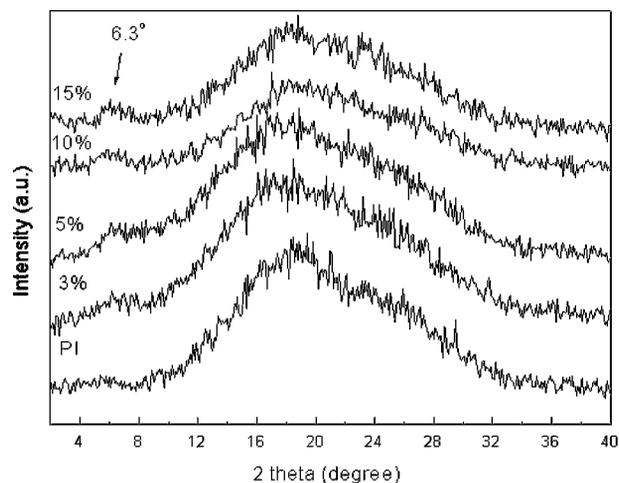

Figure 3. XRD profiles of PI/POSS nanocomposites containing various POSS.

in a semi-IPN framework are, therefore, amorphous, as evidenced by the absence of any sharp crystalline reflection in the wide-angle region of the XRD profiles. However, a broad maximum at $2\theta = 6.3°$ reveals the aggregation of POSS units in the PI/POSS semi-IPN framework. The peak intensity at $2\theta = 6.3°$ increases with the POSS content, which indicates increased aggregation. This aggregation of multifunctional methacrylated-POSS in the PI matrix is similar to that of an epoxy-POSS/epoxy system. Matejka et al.[24] reported the morphology of multifunctional epoxy-POSS that incorporates an epoxy resin. Two factors are stated to affect the morphology of the epoxy-POSS/epoxy system. These are 1) miscibility between the epoxy-POSS and the epoxy resin, and 2) the reactivity of the epoxy POSS with plain epoxy cured with a curing agent. The epoxy-amine reaction is not random and the slower incorporation of epoxy-POSS monomers into the network may result in a heterogeneous POSS distribution within the matrix. Our earlier paper[22] demonstrated that the reactivity of epoxy-POSS (E_a of OG/mPDA is $59.11\ kJ \cdot mol^{-1}$) cured with a curing agent is lower than that of plain epoxy (E_a of DGEBA/mPDA is $53.5\ kJ \cdot mol^{-1}$). In the proposed semi-IPN system, the reactivity effect is excluded and the miscibility factor may affect the morphology of the PI/POSS hybrid. The FT-IR spectra of PI/POSS that contains 15 wt.-% of methacrylated-POSS still demonstrates the disappearance of the C=C group ($\approx 1\,640\ cm^{-1}$), so the complete self-curing of the methacrylated-POSS during the imidization of PAA can be guaranteed. The self-curing of methacrylated-POSS and the imidization of PAA do not affect each other. Thus, the only factor that can influence the morphology of the PI/POSS hybrid is the miscibility between PAA and methacrylated-POSS. The FE-SEM micrographs confirm the miscibility effect. Figure 4(A−D) present FE-SEM micrographs of polyimides that contain various methacrylated-POSS contents. The uniform size of the aggregated POSS particles is approximately 50−60 nm,
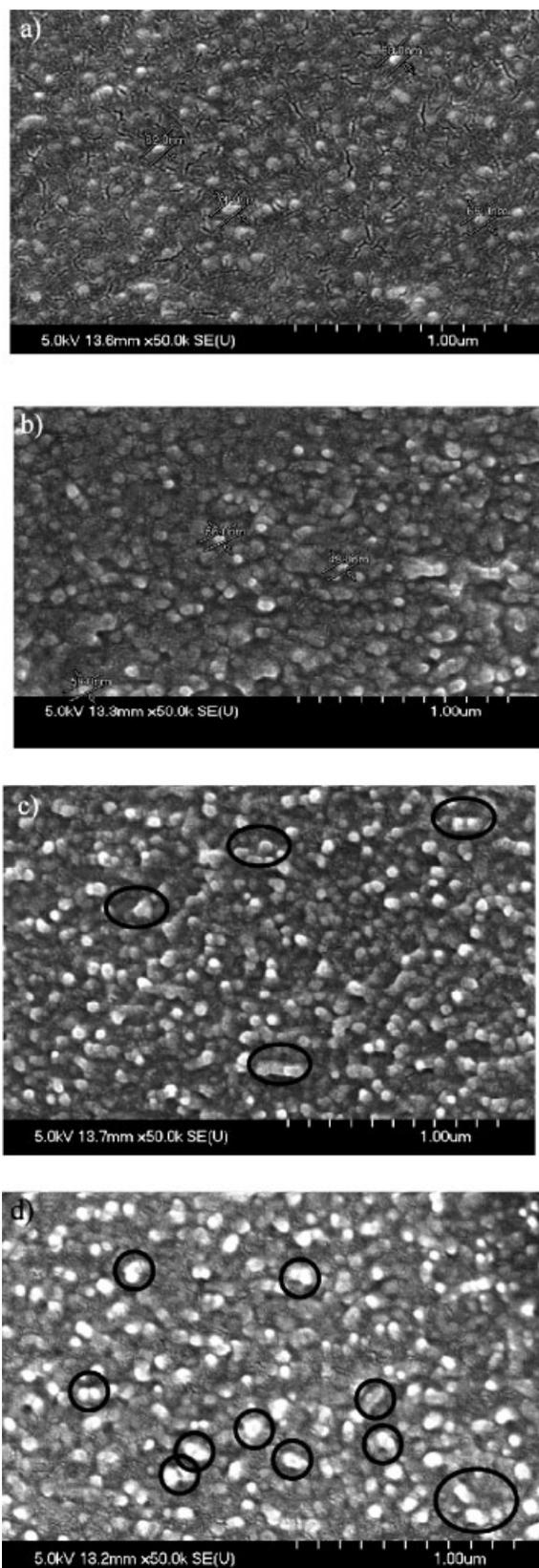
Figure 4. FE-SEM micrographs of PI/POSS nanocomposites containing various POSS: a) 3 wt.-% POSS, b) 5 wt.-% POSS, c) 10 wt.-% POSS, and d) 15 wt.-% POSS.

regardless of POSS content in the PI matrix. Those with lower methacrylated-POSS contents exhibit slight aggregation. The nanocomposites with higher methacrylated-POSS contents exhibit significant aggregation. The dramatic methacrylated-POSS aggregation in the polyimide matrix yields an interconnected phase (Figure 4(C) and (D)) among the aggregated particles. In Figure 4(C) and (D), the marked circles represent the interconnected and aggregated POSS particles in the PI matrix.

Thermal Properties

The glass transition temperature, the thermal stability, and CTE of PI/POSS semi-IPN nanocomposites are measured by DMA, TGA, and TMA, respectively, and are listed in Table 1. The plain PI exhibits a well-defined tan δ relaxation peak centered at 370.3 °C, which corresponds to the glass transition of the plain PI. The PI/POSS nanocomposites that contain 3, 5, 10, and 15 wt.-% of methacrylated-POSS also clearly exhibit a single transition at 376.1, 379.2, 384.8, and 380.4 °C, respectively. The glass transition temperature (T_g) of the nanocomposites increase with the methacrylated-POSS content up to 10 wt.-%. However, the T_g of the PI that contains 15 wt.-% methacrylated-POSS actually decreases as the methacrylated-POSS content increases. The T_g of the PI/POSS semi-IPN nanocomposites varies very similarly to that of the epoxy-POSS/epoxy system.[11] Li et al.[13] indicated that the epoxy-POSS is covalently bonded to the chain, and the cross-linking density of the epoxy/POSS hybrid is increased, which significantly slows the relaxation of the chain. The low POSS content incorporated into the epoxy resin can significantly increase the T_g of the epoxy/POSS nanocomposite, whereas the T_g associated with the high epoxy-POSS content is lower than that of the plain epoxy. Curing of the epoxy-POSS with curing agent is less efficient than for the plain epoxy resin, so the crosslinking density is lower. The semi-IPN system can significantly effect the T_g of the PI/POSS nanocomposite through the formation of cross-linked networks in a semi-IPN system (Figure 2(D)). The semi-IPN framework of the PI/POSS nanocomposite can remarkably hinder the molecular motion and enhance the T_g with the lower percentage of

Table 1. Physical properties of PI/POSS semi-IPN nanocomposites.

Code	T_g	T_{dec}[a]	CTE	Dielectric constant
	°C	°C	ppm $\cdot$ °C^{-1}	
PI	370.3	530.7	31.21	3.19
PI/3 wt.-% POSS	376.1	498.3	40.59	3.02
PI/5 wt.-% POSS	379.2	485.0	40.51	2.80
PI/10 wt.-% POSS	384.8	475.5	42.07	2.67
PI/15 wt.-% POSS	380.4	460.0	44.79	2.51

[a] 5% weight loss temperature.

cross-linked methacrylated-POSS in the polyimide matrix. However, if the composition of cross-linked methacrylated-POSS is too high, the trapped PI molecules can be squeezed out of the networks, which results in phase separation because of the poor miscibility, and the methacrylated-POSS will behave as a plasticizer to depress the T_gs of the PI/POSS nanocomposites with a higher POSS content (15 wt.-%). In addition, many phase-separated POSS molecules form large interconnected aggregated domains that can be seen in the FE-SEM micrograph. As a result, these aggregated POSS domains that have no covalent bonding with polyimide chains, behave like the fillers in the PI matrix. Thus, the plasticizing effect of POSS aggregated particles depresses the T_g of polyimides with a high concentration of methacrylated-POSS.[22] Table 1 presents the thermal stabilities in nitrogen determined from the TGA thermograms. The temperature at which 5% of the mass is lost is chosen as the degradation temperature (T_{dec}), to compare the relative thermal stabilities of the composites. The T_{dec} of plain PI is 530.7 °C. The T_{dec} of PI/POSS nanocomposites that contain 3, 5, 10 and 15 wt.-% methacrylated-POSS are 498.3, 485.0, 475.5 and 460.0 °C, respectively. The T_{dec} of the PI/POSS nanocomposite decreases as the methacrylated-POSS content increases because the methacrylated-POSS has poor thermal stability (with a T_{dec} of 350.1 °C). The coefficients of thermal expansion (size stability) of the PI/POSS nanocomposite are measured by TMA. The CTE of plain polyimide is 31.2 ppm · °C^{-1}. The CTE of the PI/POSS nanocomposites slightly increases with the POSS content. The acrylic group of the methacrylated-POSS has a high CTE, but the high cross-linking and rigid structure of POSS efficiently reduces the CTE. Therefore, the PI/POSS nanocomposite exhibits slightly less size stability than the plain polyimide.

Dielectric Property

The dielectric constants of the PI/POSS nanocomposites are measured at 100 kHz by DEA. Table 1 presents the results. The dielectric constants of the PI/POSS nanocomposites decrease steadily with methacrylate-POSS content because of the porous cage of the POSS[20,23−25] and the low k value of air (1.1). Increasing the relative porosity of polyimide efficiently reduces the dielectric constant of the PI/POSS nanocomposite. Hence, the dielectric constant of the PI/POSS nanocomposite decreases steadily as the methacrylated-POSS content increases (2.51, methacrylated-POSS 15 wt.-%).

Conclusion

Octa-acrylate polyhedral oligomeric silsesquioxane is employed to prepare polyimide-based simultaneous semi-IPN nanocomposites with a low dielectric constant and high performance in a single-step process. The DSC and FT-IR results demonstrate that the self-curing of methacrylated-POSS and the imidization of polyamic acid (PAA) occurs simultaneously. The self-curing of methacrylated-POSS occurs at almost the same time as the imidization of PAA. Therefore, a convenient way to prepare a high-performance polyimide nanocomposite is developed. The PI/POSS nanocomposite exhibits enhanced glass transition temperatures. The dielectric constant of PI/POSS nanocomposites decreases as the POSS content increases because the PI/POSS nanocomposites are much more porous than plain polyimide. A semi-IPN structure with POSS particles, with sizes of approximately 50–60 nm, uniformly embedded into polyimide matrices with various POSS contents is obtained. A high POSS content is associated with the interconnected morphology of neighboring POSS-aggregated particles.

[1] M. T. Bohr, *Solid State Technol.* **1996**, *9*, 105.

[2] G. Maier, *Prog. Polym. Sci.* **2001**, *26*, 3.

[3] K. R. Carter, R. A. DiPietro, M. I. Sanchez, S. A. Swanson, *Chem. Mater.* **2001**, *13*, 213.

[4] Q. R. Huang, W. Volksen, E. Huang, M. Toney, C. W. Frank, R. D. Miller, *Chem. Mater.* **2002**, *14*, 3676.

[5] J. J. Watkins, J. M. Blackburn, T. J. McCarthy, *Chem. Mater.* **1999**, *11*, 213.

[6] K. H. Hsieh, J. L. Han, C. T. Yu, S. C. Fu, *Polymer* **2001**, *42*, 2491.

[7] S. Marturunkakul, J. I. Chen, R. J. Jeng, J. Kumar, S. K. Tripathy, *Chem. Mater.* **1993**, *5*, 592.

[8] G. Ragosta, P. Musto, M. Abbate, P. Russo, G. Scarinzi, *Macromol. Symp.* **2005**, *228*, 287.

[9] Y. H. Zhang, Y. Lia, S. Y. Fua, J. H. Xinb, W. A. Daoudb, L. F. Lia, *Polymer* **2005**, *46*, 8373.

[10] M. Abbate, P. Musto, G. Ragosta, G. Scarinzi, L. Mascia, *Macromol. Symp.* **2004**, *218*, 211.

[11] M. A. Wahab, I. Kim, C. S. Ha, *J. Polym. Sci., Part A: Polym. Chem.* **2004**, *42*, 5189.

[12] J. Zhang, B. K. Zhu, H. J. Chu, Y. Y. Xu, *J. Appl. Polym. Sci.* **2005**, *97*, 20.

[13] G. Z. Li, L. C. Wang, H. Toghiani, T. L. Daulton, K. Koyama, C. U. Pittman, Jr., *Macromolecules* **2001**, *34*, 8686.

[14] D. Katherine, D. C. Wayne, *Macromolecules* **2002**, *35*, 7942.

[15] D. Katherine, D. C. Wayne, R. Laurent, G. Jocelyne, S. Henry, *Macromolecules* **2001**, *34*, 6623.

[16] M. S. Lin, C. C. Liu, *Polym. Int.* **1999**, *48*, 137.

[17] M. Kamal, A. K. Srivastava, *React. Funct. Polym.* **2001**, *49*, 55.

[18] J. C. Huang, C. B. He, X. M. Liu, J. W. Xu, C. S. S. Tay, S. Y. Chow, *Polymer* **2005**, *46*, 7018.

[19] H. Z. Liu, S. X. Zheng, *Macromol. Rapid Commun.* **2005**, *26*, 196.

[20] C. M. Leu, G. M. Reddy, K. H. Wei, C. F. Shu, *Chem. Mater.* **2003**, *11*, 2261.

[21] C. Zhang, F. Babonneau, C. Bonmme, R. M. Laine, C. L. Soles, H. A. Hristov, A. F. Yee, *J. Am. Chem. Soc.* **1998**, *120*, 8380.

[22] L. Matejka, A. Strachota, J. Plestil, P. Whelan, M. Steinhart, M. Slouf, *Macromolecules* **2004**, *37*, 9449.

[23] C. M. Leu, Y. T. Chang, K.-H. Wei, *Macromolecules* **2003**, *36*, 9122.

[24] W. Y. Chen, Y. Z. Wang, S. W. Kuo, C. F. Huang, P. H. Tunga, F. C. Chang, *Polymer* **2004**, *45*, 6897.

[25] Y. J. Lee, J. M. Huang, S. W. Kuo, J. S. Lu, F. C. Chang, *Polymer* **2005**, *46*, 173.

www.mrc-journal.de